Final Technical Progress Report

Report Number: FTR1

Date of Report: 12/29/06

Report Period: July 1, 2005 to September 30, 2006

Contract Title: Novel Cathodes Prepared by Impregnation Procedures

Contract Number: DE-FC26-05NT42514

Author / Principal Investigator: Eduardo Paz

Performing Organization: Franklin Fuel Cells, Inc.
83 Great Valley Parkway
Malvern, PA 19355

Subcontractor: Raymond J. Gorte and John M. Vohs
Department of Chemical & Biomolecular Engineering
University of Pennsylvania
Philadelphia, PA 19104

Disclaimer

Abstract

1) We showed that similar results were obtained when using various LSM precursors to produce LSM-YSZ cathodes.
2) We showed that enhanced performance could be achieved by adding LSCo to LSM-YSZ cathodes.
3) We have preliminary results showing that there is a slow deactivation with LSF-YSZ cathodes.

Executive Summary

A) SOFC Cathodes Prepared by Infiltration with Various LSM Precursors

The cathode properties of LSM-YSZ composites formed by infiltration of porous YSZ with aqueous salt solutions, with LSM nano-particles, and with molten salts are essentially identical. The relatively high mobility of LSM on YSZ, associated with surface interactions between LSM and YSZ, causes the final composite structures to be essentially the same, independent of how the LSM is added. Therefore, the only important factor in preparing the infiltrated electrodes is achieving the necessary LSM loading (~40 wt% LSM) in the fewest possible steps.

B) An Examination of LSM-LSCo Mixtures for Use in SOFC Cathodes

The SOFC cathode characteristics of LSM-LSCo mixtures depend strongly on how the mixtures are prepared. Mixed perovskite La0.8Sr0.2Mn(1-x)CoxO3 can be easily formed by a wet co-impregnation method. However, the composites did not show superior performance as SOFC cathodes. CoOx or LSCo can be easily introduced into LSM-YSZ composites without formation of insulating phases; however, only the addition of LSCo increased the cathode performance of the LSM-YSZ composite. Using mixtures of LSM and LSCo did not prevent the deactivation associated with reaction of LSCo and YSZ.

C) Stability Studies of LSF-YSZ Electrodes.

We have preliminary results on the deactivation of LSF-YSZ electrodes at 973 K. Ohmic losses appear to be stable after 2000 h. However, we are observing an increase in the polarization losses after this period of time. We are presently working to identify the deactivation mechanism but we believe it is associated with Zr doping of the LaFeO3.

Introduction

While the performance of conventional Sr-doped LaMnO3 (LSM)-YSZ cathodes is adequate at high temperatures, LSM-YSZ composites exhibit only modest performance at 700ºC and poor performance at lower temperatures. Since there is a move towards operation at lower temperatures, cathodes with properties superior to LSM-YSZ are clearly needed. In fact, cathode performance can be improved dramatically by replacing LSM with other perovskites, such as Sr-doped LaFeO3 (LSF) or LaCoO3 (LSCo) [1,2]. Unfortunately, it is not a simple matter to substitute these alternative perovskites for LSM. The conventional fabrication of LSM-YSZ composites involves a high-temperature calcination of LSM-YSZ mixtures to the electrolyte in order to establish good connectivity between the electrode and electrolyte. With LSM, calcination can be performed at 1250ºC, a temperature that is sufficiently high to sinter the YSZ in the electrode to the YSZ in the electrolyte, thus forming a good three-phase boundary. Unfortunately, it is not possible to calcine LSF-YSZ and LSCo-YSZ mixtures at high temperatures due to the fact that these oxides will undergo solid-state reactions.

An alternative approach to preparing composite cathodes involves eliminating high-temperature sintering of LSF (or LSCo) with YSZ. It has been pointed out that the

driving force for reaction between the perovskites and YSZ disappears below 900°C. This implies that the problem of interfacial reactions may be primarily associated with processing the composite electrode, rather than fuel-cell operation, although interfacial reaction could also occur because of the reducing conditions associated with the electrode-electrolyte interface.

Approach

One way to form an oxide composite that is well connected to the electrolyte, while avoiding the high-temperature co-firing of YSZ and perovskite, involves adding the perovskite to a porous matrix of the YSZ that has already been sintered to high temperatures. The porous YSZ matrix can be produced by simple methods, such as tape casting or tape calendaring with pore formers. The tapes with pore formers can be laminated onto electrolyte tapes in the green state and co-fired together with the green anode. Finally, the perovskite is incorporated into the porous YSZ by infiltration.

Results and Discussion

A) SOFC Cathodes Prepared by Infiltration with Various LSM Precursors

Although the infiltration approach to produce LSM-YSZ cathodes has a number of advantages, the fabrication procedure does have limitations. First, a calcination step is still required to synthesize the perovskite phase from the mixed salts. Second, the infiltration procedure can be tedious if many impregnation steps are required to achieve a reasonable perovskite loading. Since the pore volume within the YSZ matrix limits the amount of the solution that can be added, the maximum amount of solids that can be added in a single impregnation step corresponds to the equivalent volume fraction of solid in the solution. Third, it can be difficult to achieve a uniform distribution of the perovskite phase within the YSZ structure. Therefore, we set out to compare the properties of LSM-YSZ composites prepared by infiltration using aqueous solutions of nitrate salts, using LSM nano-particles, and using a "solvent-less" mixture of molten nitrate salts.

Each of the composites was prepared by infiltrating LSM into a pre-sintered, porous YSZ matrix, with the YSZ prepared using tape-casting methods. YSZ powder (Tosoh Corp., TZ-84.8% Y_2O_3, 0.2 μm) was mixed with distilled water, a dispersant (1.27 g, Duramax 3005, Rohm & Haas), binders (10.2 g HA12 and 14.4 g B1000, Rohm & Haas), and a pore former (graphite, GE, Alfa Aeser, 325 mesh, conductivity grade). The resulting slurry was cast into tapes, which could then be laminated onto other green tapes that did not have pore formers to form a porous-dense YSZ bilayer. For the measurements in this paper, the porous YSZ layer was fixed at 60 μm. After calcination to 1823 K, the porous layer was found to be approximately 65% porous, with relatively uniform pores between 1 and 2 μm in diameter. An SEM image of this layer is shown in Fig. 1a).

Three different methods were used to add the LSM to the porous YSZ. The aqueous-solution method for making the composite has been described previously [8]. Briefly, $La(NO_3)_3$ $6H_2O$ (Alfa Aesar, ACS 99.9%), $Sr(NO_3)_2$ (Alfa Aesar, ACS 99.0%), and $Mn(NO_3)_2$ xH_2O (Alfa Aesar, ACS 99.98%) were dissolved in distilled water at a

molar ratio of La:Sr:Mn=0.8:0.2:1 to give a solution with a $La3^{+}$ molarity of 1.6 mol/l. The solution was then added at room temperature to the porous YSZ matrix, which was then dried and heated to 723 K to decompose the nitrate ions and form the mixed oxides. After cooling the samples back to room temperature, the impregnation steps were repeated 4 or 5 times until the loading of mixed oxides corresponded to 40-wt% LSM. Finally, the composite was calcined at 1323 K to form the perovskite phase. This sample will be referred to as LSM-YSZ(aq).

The second method for adding LSM to the porous YSZ involved impregnation with a colloidal dispersion of LSM nano-particles. The clear nano-particle solution (MetaMateria Partners, Columbus, OH 43212) was 20-wt% $La_{0.85}Sr_{0.15}MnO_x$ in a 1,4 butanediol solvent. It was again necessary to use multiple impregnations to achieve 40-wt% LSM, with removal of the solvent by heating in air at 723 K between each step. Based on the volume of solution that could be added to the porous YSZ in each step, we estimated that it should take approximately 14 impregnations to reach the target loading; however, in practice, we found it necessary to perform more than 20 impregnation steps. Finally, the LSM-YSZ composite, referred to here as LSM-YSZ(nano), was calcined to 1323 K to sinter the nano-particles.

The third method for adding LSM to the porous YSZ took advantage of the low melting temperatures for $La(NO_3)6\ H_2O$ (313 K) and $Mn(NO_3)_2\ 4H_2O$ (299 K). These two salts were mixed in a La:Mn molar ratio of 0.9, then melted at approximately 353 K to form a clear liquid. $Sr(NO_3)_2$ (T_{mp} = 843 K) was then added to the molten salt solution at a Sr:Mn ratio of 0.1, together with a very small amount of distilled water so as to get the Sr salt to dissolve completely. The molten salt was then added to the porous YSZ and heated to 723 K in air to decompose the nitrate. Only two impregnation steps were required to achieve a loading of 35-wt% of the LSM precursor. The LSM perovskite phase formed after calcination in air at 1323 K for 2 h and the composite will be referred to as LSM-YSZ(molten).

One would notice that the strontium doping level is 15% in the LSM-YSZ(nano) sample. This is due to the sample availability from the supplier. In the LSM-YSZ (molten), strontium molar fraction is only 10%. The electrochemical properties of $La_{1-x}Sr_xMnO_3$ oxides could be changed when doping level is varied. Many studies have shown that with Sr doping $0.1<x<0.3$, the electrical conductivity of $La_{1-x}Sr_xMnO_3$ is in the range of 100~200 S/cm. The oxygen diffusion coefficients for $LaMnO_3$-based perovskites are scattered over one or two orders of magnitude from the literature. However, those values for diffusivity are still very low compared with the values required for mixed conducting oxides. Essentially, the electrical conductivity and catalytic activity of LSM in this work are very similar despite the different Sr doping fraction.

The electrochemical properties of the composites were tested at 973 K on anode-supported fuel cells that had a 60-µm thick electrolyte and a 300-µm anode. The anode in each of these cells was also prepared by impregnation of porous YSZ to a loading of 15-wt% CeO_2 and 30-wt% Co, using aqueous nitrate salts solutions. The active area of the cells was 0.35 cm^2. During the testing, humidified H_2 (3% H_2O) was fed to the anode and the cathode was simply exposed to air. The electronic contacts were made using Ag wire and Ag paste on the cathode and Au wire with Au paste on the anode. Each fuel cell was sealed onto a 1.0-cm alumina tube using a ceramic adhesive (Aremco, Ultra-Temp 516). All impedance data were recorded in the galvanostatic mode, using a Gamry Instruments

Potentiostat, with a frequency range from 0.01 Hz to 100 kHz and a 10 mA perturbation. Before characterizing the electrochemical performance of the cells, they were briefly shorted in order to activate the LSM.

Samples for the AFM measurements were prepared by diluting the aqueous solution of La, Sr, and Mn salts by 100 times with distilled water, then spraying that solution onto YSZ(100) single crystals (MTI Corporation) to form small LSM particles. The spraying was performed using an air brush while holding the YSZ crystals at approximately 370 K on a hot plate. The crystals were then calcined in air to 1123, 1323, or 1423 K, temperatures sufficient to form the perovskite phase from the mixed salts, and characterized using atomic force microscopy (AFM). Because the LSM deposition method that we used did not provide a uniform distribution of particles, the data that is shown in this paper were taken on the same sample, after heating to sequentially higher temperatures, using our best efforts to examine the same part of the crystal in each case. However, the general observations that will be reported here were representative of what was observed on all samples that were examined. The AFM experiments were performed in air using a Digital Instruments Nanoscope operated in the tapping mode.

The LSM-YSZ composites were initially characterized using XRD and SEM. The XRD patterns on each of the composites were identical and indistinguishable from traditional LSM-YSZ composites. After calcination at 1323 K, the only significant peaks in the XRD were associated with YSZ and LSM. The peaks associated with LSM were somewhat broad because of the small average crystallite size, but there was no evidence for extra phases or for amorphous material in any of the samples. The SEM results for each of the composites were also indistinguishable, with results for the sample made with nano-particles (LSM-YSZ(nano)) and with the molten salts (LSM-YSZ(molten)) shown in Figs. 1b) and 1c) for a final calcination at 1323 K. By comparison with the empty pores (Fig. 1a)), the LSM appears as 0.1 to 0.2-μm particles that coat the walls of the YSZ. As discussed in a previous paper, the LSM particles undergo structural changes with increased calcination temperature, but these changes were the same for the composites made using different methods.

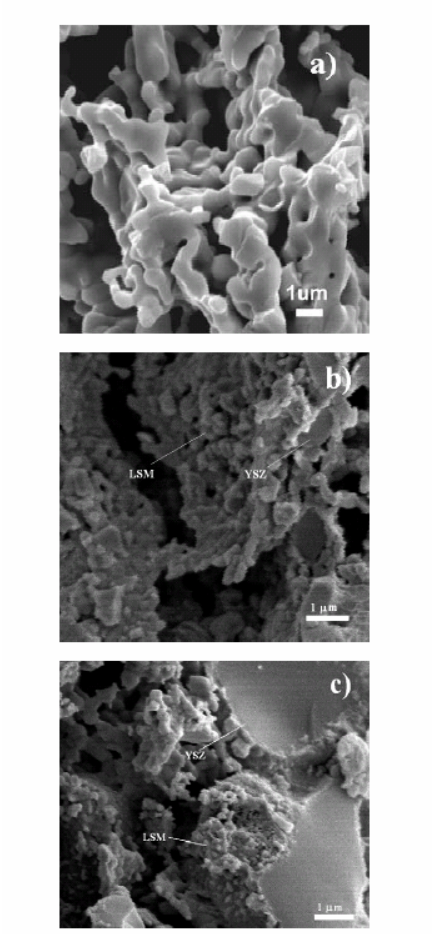

Fig. 1 SEM images of a) the initial porous YSZ matrix; b) the LSM-YSZ composite prepared by infiltration of the LSM nano-particle suspension; c) the LSM-YSZ composite prepared by impregnation of LSM molten salts.

Fig. 2 shows the performance characteristics of fuel cells at 973 K with each of the different LSM-YSZ composite cathodes, with the V-i polarization curves shown in Fig. 2a) and the impedance results shown in Fig. 2b). Based on previous work, we have estimated that the Co-ceria-YSZ anode contributes an impedance of approximately 0.2 $O.cm^2$, independent of current density. The resistance associated with the electrolytes in each of the cells is predicted to be above 0.3 $O.cm^2$, in reasonable agreement with the observed high-frequency impedance between 0.35 and 0.40 $O.cm^2$ observed in Fig. 2b). Therefore, it is straightforward to extract the performance of the cathodes from these data.

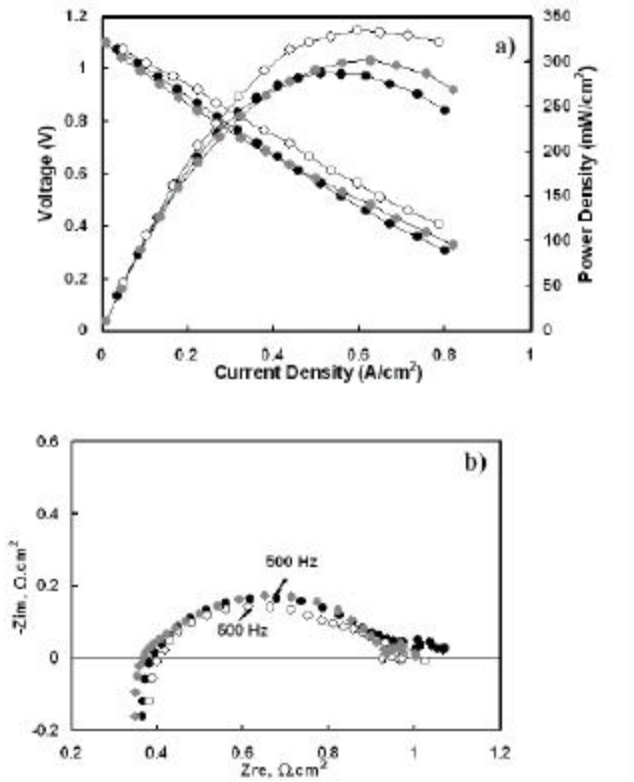

Fuel-cell data for cells operating in humidified H_2 (3% H_2O) at 973 K with LSM-YSZ cathodes prepared using different impregnation methods, followed by calcination at 1323 K: a) V-i Polarization curves; b) Cole-Cole plots of impedance data measured in humidified H_2 (3%H_2O) at 973 K at 300 mA/cm^2. (●) LSM-YSZ(aq); (●) LSM-YSZ(nano); (○) LSM-YSZ(molten).

The performance characteristics of the three cells with different cathodes are very similar. The cell with the cathode made from the molten salt, LSM-YSZ(molten), exhibited a slightly higher maximum power density, 330 mW/cm2 compared to 300 mW/cm^2 for the LSM-YSZ(nano) cell and 280 mW/cm^2 for the cell made with aqueous salt solutions (LSM-YSZ(aq)); however, this difference is within the range of variability that we observe between cells. Although the LSM-YSZ(molten) cell had a slightly lower LSM concentration, 35-wt% LSM compared to 40-wt% LSM for the other two cells, previous work with cells made using aqueous-salt impregnation of LSM showed negligible differences for LSM loadings between 30 and 40 wt%. All other physical characteristics of the LSM-YSZ composites were indistinguishable. In agreement with the slopes of the V-i curves, the Cole-Cole plots show total cell impedances, the intercept with the real axis at low frequency, between 1.0 and 1.1 O.cm^2 on each of the cells. Based on the anode and electrolyte estimates, each of the LSM-YSZ composite cathodes exhibits a loss of between 0.4 and 0.5 O.cm^2.

AFM measurements of LSM particles on a YSZ(100) crystal help to explain why the results are so similar when LSM is impregnated into YSZ using different methods. Fig. 3 provides images of LSM particles on the crystal after calcination at 1123, 1323, and 1423 K, along with line scans to show the heights of the features. The image at 1123 K (Fig. 3a)) shows that the particles were initially approximately 0.1-μm in size and

mostly of irregular shape, although some particles begin to show a rectangular shape. The particles are roughly 30 nm in height. After heating to 1323 K (Fig. 3b)), the particles doubled in size and became rectangular in shape. Interestingly, the height of the particles has not changed significantly. Based on the symmetry of the particles and the fact that they are aligned in the same directions, we suggest that the cubic perovskite particles are essentially epitaxial with the (100) surface of the YSZ single crystal, implying that there is a strong interaction between the two oxides. The most interesting result was obtained after heating to 1423 K, Fig. 3c). At this temperature, all of the particles grew and "flattened" out over the surface. The height of the spherical particles is now only 5 nm and there is evidence at the edges that the oxide is spreading out over the substrate. This would suggest that the LSM essentially "wets" the YSZ.

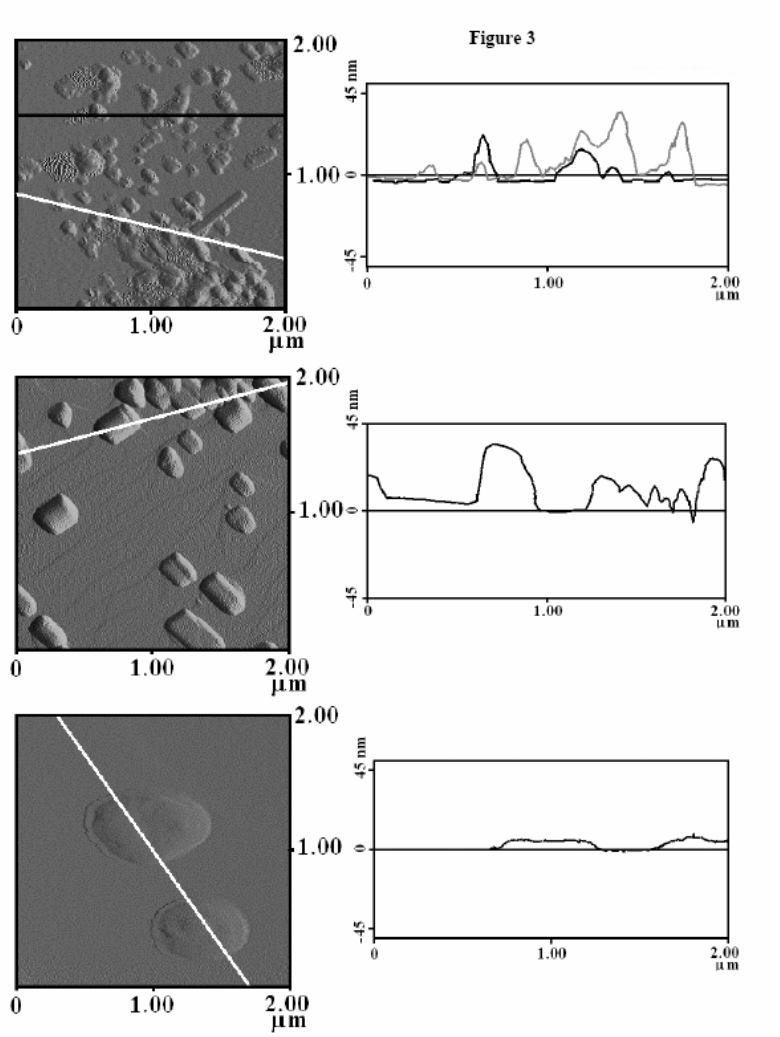

Fig. 3. 2 µm × 2 µm AFM images collected in the tapping mode of LSM particles on YSZ(100) sample after annealing in air at the following temperatures: a) 1123 K; b) 1323 K; c) 1423 K.

We had previously suggested that LSM forms a coating over YSZ in LSM-YSZ composites calcined above 1323 K based on BET surface area measurements. Furthermore, we suggested that this coating was responsible for the high impedance observed with LSM-YSZ cathodes prior to activation by polarization. In that study, LSM-

YSZ composites calcined at 1123 K were not activated by polarization. The fact that LSM spreads over the YSZ crystal at approximately the same temperature at which LSM-YSZ composites change when polarized provides further evidence that a "wetting-dewetting" phenomenon is responsible for polarization activation.

For the present study, it is more important to consider that the LSM is relatively mobile on the YSZ surface. In part, this mobility is probably driven by the same surface energies that cause the LSM to spread over the YSZ surface. What the mobility implies is that there are strong driving forces to cause the LSM-YSZ structure to evolve to the same final state for composites prepared by infiltration, independent of how one adds LSM to the YSZ. This agrees with our observations for the performance of LSM-YSZ composite cathodes.

While the final structures of the LSM-YSZ composites may be essentially independent of how the LSM is infiltrated, there clearly are practical advantages for each method. In the case of the nano-particles, it is probably still necessary to calcine the composite to sinter the particles but there is no requirement for forming the perovskite structure. If the concentration of the nano-particle solution can be made high enough, it may also be possible to use a single infiltration step. With infiltration of molten salts, the absence of a solvent eliminates the need to remove the solvent by drying. Because the drying process will tend to bring dissolved salts and nano-particles out of the pore structure, back to the external surface, it should be easier to maintain a good distribution of the LSM all the way to the electrolyte interface. The LSM distribution was not an issue with the relatively thin composites we prepared in the present study but it will likely be more important for thicker electrodes, such as one might need to prepare for cathode-supported cells.

B) An Examination of LSM-LSCo Mixtures for Use in SOFC Cathodes

One approach for modifying the electrochemical properties of LSM-YSZ composites, while maintaining their chemical and thermal stability, involves impregnating the composite with a "promoter". Recently, the group at LBL reported that the impregnation of Co, with at least some of that Co present as Co_3O_4, could be used to improve LSM-YSZ cathodes. Therefore, we set out to examine the effect of adding various Co species into LSM-YSZ cathodes.

The impregnated electrodes were again prepared by the addition of nitrate-salt solutions to porous YSZ matrices. The porous YSZ was fabricated from a slurry consisting of YSZ powder (Tosoh Corp., TZ-84.8% Y2O3, 0.2 μm), mixed with distilled water, dispersant (Duramax 3005, Rohm & Haas), binders (HA12 and B1000, Rohm & Haas), and pore formers (graphite). The slurry was cast into the desired shape, either as a tape for laminating onto a second electrolyte tape that did not contain pore formers or as rectangular blocks for other measurements. After calcination at 1823 K, the YSZ was found to have porosity between 65% and 70%, as determined by water uptake measurements. Scanning electron microscopy (SEM) showed that the pores were almost uniform in size, approximately 1.5 μm in diameter.

To prepare the perovskite composites, aqueous solutions of $La(NO_3)_3\ 6H_2O$, $Sr(NO_3)_2$, $Mn(NO_3)_2\ xH_2O$, and $Co(NO_3)_3\ 6H_2O$ (each of the salts obtained from Alfa Aesar) were added to the porous YSZ at the appropriate molar ratio, followed by drying

at ~373 K and decomposition of the nitrate ions at 723 K. With the exception of the Co-impregnated sample, all samples in this study contained 40-wt% of the perovskite phase. In all of the samples, the Sr doping corresponded to substitution of 20% of the A (La) sites in the perovskite structure. Those samples containing the mixed perovskite were made by simultaneous impregnation of $Mn(NO_3)_2$ xH_2O and $Co(NO_3)_3$ $6H_2O$ and will be designated by the percent of Co in the B sites (e.g., LSMC10 corresponds to $La_{0.8}Sr_{0.2}Mn_{0.9}Co_{0.1}O_3$). Samples in which $Co(NO_3)_3$ $6H_2O$ or mixtures of $La(NO_3)_3$ $6H_2O$, $Sr(NO_3)_2$, and $Co(NO_3)_3$ $6H_2O$ were added to an existing LSM-YSZ composite will be described separately.

After reaching a loading of 40-wt% for the impregnated oxide, a final calcination step to higher temperatures was required to produce the perovskite phase, with the perovskite phase formed at 973 K with $La_{0.8}Sr_{0.2}CoO_3$ (LSCo) and at 1123 K with $La_{0.8}Sr_{0.2}MnO_3$ (LSM). LSCo-YSZ composites performed well as SOFC cathodes following calcination between 973 and 1173 K but showed poor performance after treatment at higher temperatures due to solid-state reactions. By comparison, LSM-YSZ composites performed poorly following calcination at 1123 K, exhibiting optimal performance only after heating above 1323 K. Therefore, to make a fair comparison of the mixed perovskites, we chose to study samples prepared at both 1173 and 1373 K, with the idea that one of these temperatures is likely to be optimal for all compositions. The phases of all the composites were evaluated by XRD using a monochromated Cu Ka radiation source.

The electrochemical properties of the composites were tested on anode-supported, button cells; however, earlier studies have shown that area-specific parameters are independent of cell size. All button cells consisted of a ~300-µm thick anode with 15-wt% CeO_2 and 30-wt% Co, prepared by impregnation of aqueous nitrate salts solutions. Both the electrolyte and cathode layers were 60-µm thick. The electronic contacts were made using Ag wire and Ag paste on the air electrodes and Au wire with Au paste on the electrodes exposed to H_2. Each fuel cell was sealed onto a 1.0-cm alumina tube using a ceramic adhesive (Aremco, Ultra-Temp 516). All impedance data was recorded in the galvanostatic mode, using a Gamry Instruments Potentiostat, with a frequency range from 0.01 Hz to 100 kHz and a 10 mA perturbation. Before characterizing the electrochemical performance of the cells, they were briefly shorted. With the LSM-YSZ cathodes, this step was necessary in order to avoid artifacts associated with polarization activation.

XRD results for the LSMC-YSZ, LSM-YSZ, and LSCo-YSZ composites calcined at 1173 K in air are shown in Fig. 4 for the region between 29 and 34 degrees 2?. In each case, calcination at 1173 K was sufficient to form the perovskite phase. All of the samples showed broad peaks, partly due to the fact that the crystallites making up the perovskite phase were small and partly due to LSM having an orthorhombic structure. Because the diffraction peaks for LSMC shift continuously with the fraction of Co in the B site, the mixed perovskites must be forming, rather than separate LSM and LSCo phases. There was no evidence for excess La_2O_3 or $La(OH)_3$ within the detection limit of the equipment (~2%).

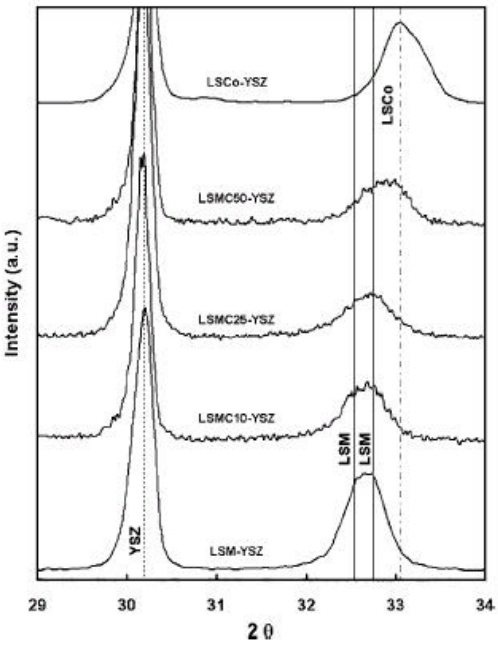

Fig. 4. XRD patterns of YSZ-$La_{0.8}Sr_{0.2}Mn_{(1-x)}Co_xO_3$ (x = 0, 0.1, 0.25, 0.5. and 1.0) composites prepared by impregnation after calcination at 1173 K.

Fig. 5a) shows V-I performance curves for the anode-supported cells operating in humidified H_2 (3% H2O) at 973 K with LSM-YSZ and LSMC-YSZ cathodes. Data for the cell with an LSCo-YSZ cathode, using the same Co-based anode, is not included here but showed a maximum power density of 0.48 W/cm^2. All of the cells achieved an open-circuit voltage (OCV) of 1.1 V and the cell potentials decreased linearly with the current density up to 0.7 A/cm^2. The differences between the cells made with LSM, LSMC10, and LSMC50 were negligible, with each exhibiting a maximum power density of approximately 250mW/cm^2. Only the cell made with LSMC25 showed significantly better performance, with a maximum power density of 305mW/cm^2.

The impedance data for each of these cells, measured at OCV and shown as Cole-Cole plots in Fig. 5 b), also demonstrate that the LSMC25 cathode exhibits the best performance. The ohmic resistance in each cell, determined from the high-frequency intercept with the real axis, was approximately 0.45 O.cm^2, a value somewhat higher than that calculated for the 60-µm electrolyte, using 0.021 S/cm as the conductivity for YSZ at 973 K. Since identical cells with LSCo cathodes exhibited a total polarization loss, determined from the span under the arcs in the Cole-Cole plot, of 0.25 O.cm2 under identical conditions, the anode contribution to the cell losses cannot be greater than approximately 0.2 O.cm^2. Therefore, most of the polarization losses in Fig. 5b) are associated with the cathodes. With the LSMC25 cathode, these losses are approximately 0.35 O.cm^2; with the other materials, the cathode impedances are approximately 0.55 O.cm^2.

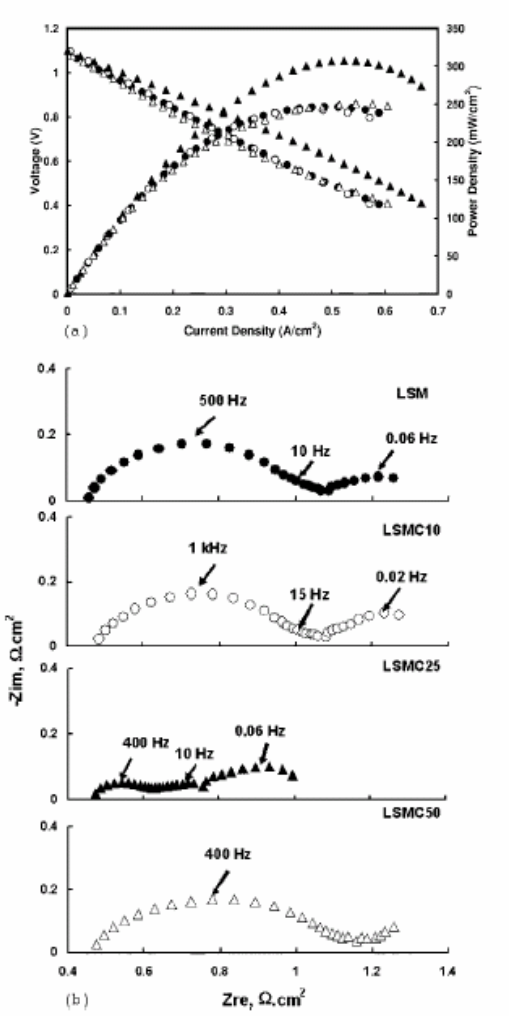

Fig. 5. a) V-i performance curves for anode-supported cells with Co-ceria-YSZ anodes measured in humidified (3% H_2O) H_2 at 973 K using $La_{0.8}Sr_{0.2}Mn_{(1-x)}Co_xO_3$-YSZ (x = 0, 0.1, 0.25, and 0.5)composite cathodes prepared by impregnation and calcination at 1173 K. b) Impedance spectra for the same anode-supported cells, measured at OCV. The cathodes for these cells were as follows: ●, LSM-YSZ; ○, LSMC10-YSZ; ▲, LSMC25-YSZ; ?, LSMC50-YSZ.

As mentioned earlier, LSM-YSZ cathodes prepared by impregnation exhibit better performance following calcination at 1373 K while LSCo-YSZ cathodes undergo deactivation after calcination at 1373 K. Therefore, we examined the LSMC-based cathodes following the treatment at higher temperatures. The XRD results for each of the impregnated perovskites are shown in Fig. 6. Again, the diffraction results are consistent with formation of the mixed, LSMC perovskites, with no evidence for segregation to LSM and LSCo phases. However, as with LSCo-YSZ composites, there is evidence for new diffraction peaks associated with $La_2Zr_2O_7$ and SrZrO3 for the LSMC25 and LSMC50 samples after the treatment at 1373 K.

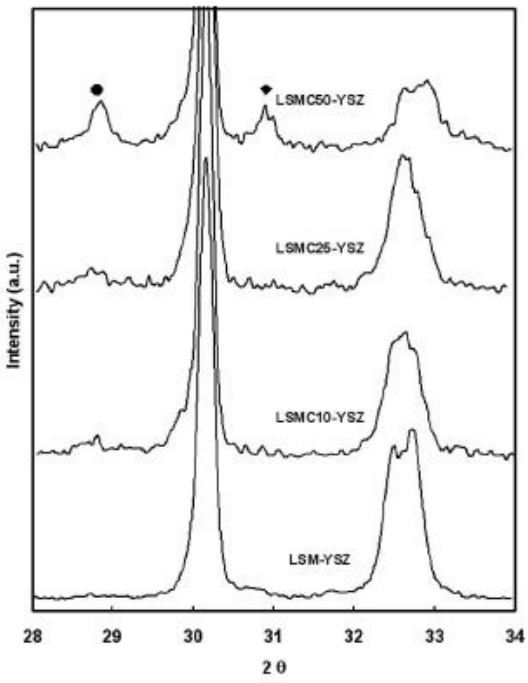

Fig. 6. XRD patterns of YSZ-$La_{0.8}Sr_{0.2}Mn_{(1-x)}Co_xO_3$ (x = 0, 0.1, 0.25, and 0.5) composites prepared by impregnation after calcination at 1373 K. In addition to the perovskite phase, peaks associated with $La_2Zr_2O_7$ (●) and $SrZrO_3$ (◆) were observed.

The V-I polarization curves for the anode-supported cells measured at 973 K in humidified H_2 are shown in Fig.7a). As before, each cell exhibited a nearly linear decrease in potential with current density up to 0.6 A/cm^2. However, the best performance was now observed with the LSM-YSZ composite, with this cell showing a maximum power density of 290 mW/cm^2. While the LSM cathode improved with the increased calcination temperature, the performance of the LSMC25 was worse and the LSMC10 and LSMC50 were largely unchanged following the higher-temperature treatment.

The reasons behind the performance changes are revealed by the AC impedance results, measured at OCV and shown in Fig. 7b). First, the ohmic resistance of the cell with LSM-YSZ cathode decreased by approximately 0.1 O.cm^2 after the 1373-K heat treatment; indeed, the new value for the ohmic resistance is close to that which would be expected for a 60-µm, YSZ electrolyte. The higher sintering temperature improves the electronic conductivity of the LSM-YSZ composite, probably by decreasing the grain-boundary resistance. Of more interest here is the fact that the ohmic losses for each of the LSMC samples are higher than for the LSM cell and that these ohmic losses increase with Co content, up to a value of 0.55 O.cm^2 for the LSMC50 sample. This increased ohmic resistance is likely associated with the formation of $La_2Zr_2O_7$ and $SrZrO_3$ produced by the solid-state reaction between perovskite and YSZ. The overall performance of the LSMC25 and LSMC50 samples remains comparable to that of the LSMC10 sample only because the non-ohmic losses are somewhat less.

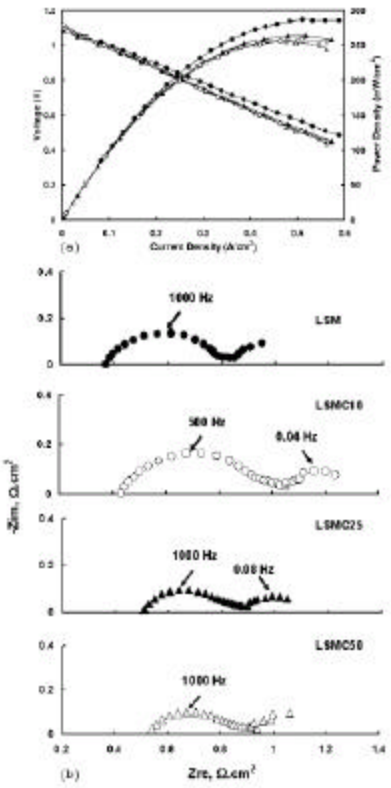

Fig. 7. a) V-i performance curves for anode-supported cells with Co-ceria-YSZ anodes measured in humidified (3% H_2O) H_2 at 973 K using $La_{0.8}Sr_{0.2}Mn_{(1-x)}Co_xO_3$-YSZ (x = 0, 0.1, 0.25, and 0.5)composite cathodes prepared by impregnation and calcination at 1173 K. b) Impedance spectra for the same anode-supported cells, measured at OCV. The cathodes for these cells were as follows: ●, LSM-YSZ; ○, LSMC10-YSZ; ▲, LSMC25-YSZ; ?, LSMC50-YSZ.

Given that electrode stability is equally important as electrode performance, the fact that the mixed perovskites underwent solid-state reaction with YSZ and showed poorer performance than LSM alone after 1373-K calcination suggests that those materials are not promising. However, composites with separate LSM and LSCo phases should be expected to exhibit performance quite different from that of the mixed perovskites; furthermore, CoO_x has been reported to enhance the performance of LSM-YSZ cathodes. Since our earlier studies of LSM-YSZ composites suggested that LSM spreads over the YSZ after calcination at higher temperatures, the LSM might prevent the solid-state reactions that occur upon contact between LSCo and YSZ.

To avoid forming the mixed perovskite with Co-containing composites, we prepared materials in which either CoOx or LSCo was added after formation of the LSM-YSZ composite. The LSM-YSZ composites were prepared with 30-wt% LSM and were calcined to 1373 K, after which 10-wt% of either Co_3O4 or LSCo were added by wet impregnation using aqueous solutions of the nitrate salts. Other than taking the cells up to the 973 K operating temperature, no additional calcination was performed after the addition of CoO_x or LSCo; however, it has been shown that this temperature is sufficient to form the perovskite, LSCo phase from the La, Sr, and Co nitrate salts. The use of 30-wt% LSM was based on our earlier finding that cathodes prepared with either 30 or 40-

wt% LSM showed similar performance, together with the goal of examining materials in which the total loading of additives was kept constant.

Fuel-cell data for the LSM-based cathodes, with and without the addition of CoO_x or LSCo, are shown in Fig. 8, with the V-i polarization curves given in Fig. 8a) and the impedance spectra in Fig. 8b). In agreement with previous results, the performance of the cell with the cathode consisting of 30-wt% LSM in YSZ was indistinguishable from that of a cell with 40-wt% LSM. The maximum power density in humidified H_2 at 973 K was again 290 mW/cm^2 and the impedance spectrum is very similar to that for LSM-YSZ in Fig. 7b). The addition of CoO_x had a negligible effect on both the V-i curve and the impedance spectrum. The slight decrease in performance at high current densities might indicate some pore blockage, but this effect is very small.

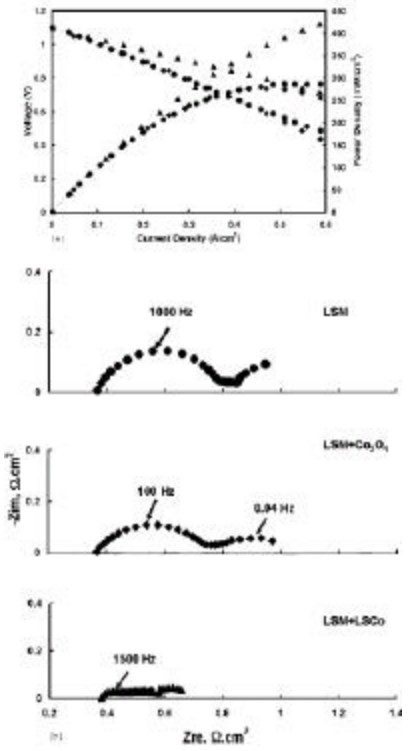

Fig. 8. a) V-I performance curves for anode-supported cells, with Co-ceria-YSZ anodes, measured in humidified (3% H_2O) H_2 at 973 K using LSM-YSZ, LSM+CoO_x-YSZ, and LSM+LSCo-YSZ composite cathodes prepared by impregnation. LSM in all the composites was calcined at 1373 K. The additional CoO_x and LSCo were impregnated into the existing LSM-YSZ and simply heated up to 973K. b) Impedance spectra for the same cells as in a), measured at OCV. The cathodes for these cells were as follows: ●, LSM-YSZ; ◆, LSM+CoO_x-YSZ; ▲, LSM+LSCo –YSZ.

However, the addition of LSCo to the LSM-YSZ affected the performance dramatically. The maximum power density increased to well above 400 mW/cm^2, and the non-ohmic losses in the impedance spectrum decreased from greater than 0.6 O.cm^2 to approximately 0.3 O.cm^2. Indeed, the performance characteristics of the cell with 10-wt% LSCo on LSM-YSZ were similar to that of a cell with only LSCo at a loading of 35-wt%.

Unfortunately, the performance of cells in which LSCo was impregnated onto LSM-YSZ was not stable. In a 250-h fuel-cell test at 973 K, there was no change in the

maximum power density during the first 150 h; however, the power density declined by approximately 25% in the next 100 h. This is an improvement over the stability of an LSCo-YSZ cathode. In that case, the decline in performance began immediately, decreasing by 25% in the first 100 h.

While we cannot definitely answer the question about why LBL workers observed large enhancements in performance upon the addition of CoO_x to an LSM-YSZ cathode, the fact that we did not observe any effect of adding CoOx, but saw large enhancements upon the addition of LSCo, at least suggests that LSCo may be the important species. The ease with which $LaCoO_3$ forms when mixtures of $La(NO_3)_3$ and $Co(NO_3)_2$ are heated together implies that perovskite phase might well form easily upon the addition of $Co(NO_3)_2$ to LSM if there were any excess La_2O_3 present. Detecting the LSCo perovskite in the presence of excess LSM would also be very difficult. We acknowledge that it is also possible that our impregnation of CoO_x may not have been as effective in forming well dispersed oxide particles in the region of the three-phase boundary, so that a final answer for this question will await further study.

The ultimate question is whether it is feasible to take advantage of Co doping to enhance the performance of LSM-YSZ cathodes. Our results suggest that LSCo has such a strong tendency to react with YSZ and form insulating phases that stability issues need to be addressed before one can answer this definitively. Assuming that the active component is LSCo, it may well be the case that stability will depend on the manner in which LSCo is added. For example, good stability might be achieved if the addition of LSCo can be controlled so that it is in contact only with the LSM, not with YSZ, although this further assumes that enhanced performance could be achieved without contact between LSCo and YSZ.

C) Stability Studies of LSF-YSZ Electrodes

This work is still ongoing but recent data obtained with a "symmetric" cell appears to be the most reliable information we have on the stability of the LSF-YSZ electrodes. This data is shown in Fig. 9 and indicates that the ohmic resistance of the cell does not change over a period of almost 1700 h. That is very encouraging, since any solid-state reactions at the interface between the electrolyte and the electrode would be expected to form insulating layers that would result in an increased ohmic resistance. However, significant increases have occurred in the electrode polarization losses. We are still attempting to definitively identify the mechanism for this deactivation, it appears that it is due to Zr doping of the $LaFeO_3$ structure.

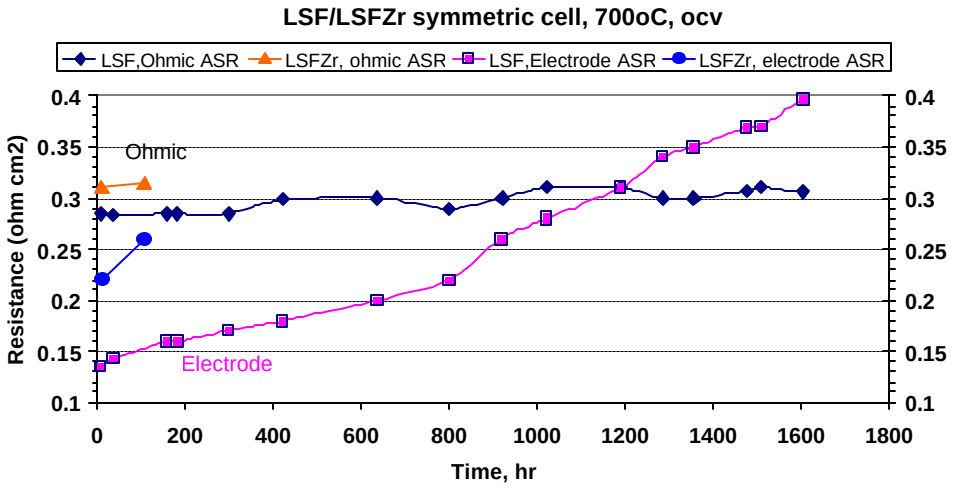

Fig. 9 Results from a "symmetric" cell, using one of the LSF-YSZ electrodes as a support. One of the LSF-YSZ electrodes is 300 microns thick, while the other is 50 microns. The electrolyte is approximately 70 microns thick. The data in the figure shows the total ohmic and polarization resistances, divided by two to account for the two electrodes.

The first evidence for this is from intentionally forming a Zr-doped LSF, $La_{0.8}Sr_{0.2}Fe_{0.9}Zr_{0.1}O_{3-d}$. XRD of the powder, Fig. 10, shows that we form the perovskite structure. This performance of an electrode made from this powder (Fig. 9) shows an increased polarization, very similar to the deactivated LSF-YSZ electrode. The ohmic resistance of the Zr-doped electrode is good, but the polarization losses are higher. What we believe is occurring is that the LSF is losing its ionic conductivity but not its electronic conductivity. An implication of this is that the performance loss should stabilize once the ionic conductivity is no longer significant.

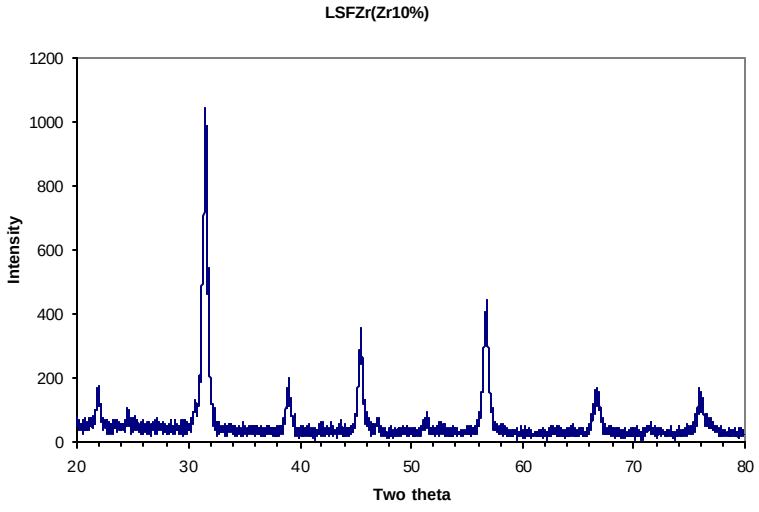

Fig. 10 XRD of the Zr-doped LSF.

Conclusion

In the one year of working under this grant, we have answered several important questions about cathodes prepared by impregnation. We have demonstrated that LSM-YSZ electrodes can be prepared from several precursors, including nanoparticles and molten salts, and that each of these precursors results in electrodes with essentially identical performance characteristics. We have found that the addition of CoOx to LSM-YSZ electrodes does not enhance the cathode performance but the addition of LSCo to LSM-YSZ electrodes can provide a significant enhancement. Unfortunately, the LSCo-enhanced electrodes are not thermally stable. Finally, we have demonstrated that LSF-YSZ electrodes undergo a slow deactivation at 973 K but the mechanism for this deactivation is not yet certain.

References

1. A. Mineshige, M. Kobune, S. Fujii, Z. Ogumi, M. Inaba, T. Yao, and K. Kikuchi, J. of Solid State Chem., 142, 374 (1999).
2. H. Uchida , S. Arisaka, and M. Watanabe, Solid State Ionics, 135, 347 (2000).2.

List of Acronyms and Abbreviations

LSM – Strontium doped lanthanum manganite
LSF – Strontium doped lanthanum ferrite
LSCo – Strontium doped lanthanum cobaltite
YSZ – Yttria stabilized zirconium oxide
$O.cm^2$ – ohm * square centimeter
h – hour
°C – Degrees celcius
Co – Cobalt
Ag – Silver
Sr – Strontium
La – Lanthanum
Mn – Manganese
Fe - Iron
Ceria – Cerium oxide